Electronic Supplementary Information

for

Cobalt entrenched N-, O-, and S-tridoped carbons as efficient multifunctional sustainable catalysts for base-free selective oxidative esterification of alcohols

Devaki Nandan, Giorgio Zoppellaro, Ivo Medřík, Claudia Aparicio, Pawan Kumar, Martin Petr, Ondřej Tomanec, Manoj B. Gawande,* Rajender S. Varma and Radek Zbořil*

Regional Centre of Advanced Technologies and Materials, Department of Physical Chemistry, Faculty of Science, Palacký University Olomouc, Šlechtitelů 27, 783 71 Olomouc, Czech Republic

* Corresponding authors: manoj.gawande@upol.cz (Manoj B. Gawande); radek.zboril@upol.cz (Radek Zbořil)

Material: Carrageenan (99.9%), urea (98%), and cobalt nitrate hexahydrate (99.9%) and alcoholic substrate were purchased from Sigma-Aldrich and were used as received without further purification. All solvents used were of HPLC grade.

Characterization: Powder X-ray diffraction (XRD) patterns of material were determined by X'Pert PRO MPD diffractometer (PANalytical) in the Bragg–Brentano geometry, equipped with an X'Celerator detector, and programmable divergence and diffracted beam antiscatter-slits at room temperature using iron-filtered Co-Kα radiation (40 kV, 30 mA, λ = 0.1789 nm). The angular range of measurement was set as 2θ = 5–90°, with a step size of 0.017°. The identification of the crystalline phases in the experimental XRD pattern was obtained using the X'Pert High Score Plus software that includes a PDF-4+ and ICSD databases. SRM660 (LaB_6) standard was used to evaluate the instrumental broadening. The X-ray diffraction lines were modelled using pseudo-Voigt functions, and single-split asymmetry correction was introduced. Additional quantitative analysis and determination of the crystalline domain sizes were performed on sample Co@NOSC using the Rietveld method. Microscopic TEM images were obtained by HRTEM TITAN 60-300 with X-FEG type emission gun, operating at 80 kV. This microscope is equipped with Cs image corrector and a STEM high-angle annular dark-field detector (HAADF). The point resolution is 0.06 nm in TEM mode. The elemental mappings were obtained by STEM-energy dispersive X-ray spectroscopy (EDS) with acquisition time 20 min. For HRTEM analysis, the powder samples were dispersed in ethanol and ultrasonicated for 5 min. One drop of this solution was placed on a copper grid with holey carbon film. XPS surface investigation has been performed on the PHI 5000 VersaProbe II XPS system (Physical Electronics) with monochromatic Al-Kα source (15 kV, 50 W) and photon energy of 1486.7 eV. Dual beam charge compensation was used for all measurements. All the spectra were measured in the vacuum of 1.3×10^{-7} Pa and at the room temperature of 21 °C. The analyzed area on each sample was a spot of 200 μm in diameter. The survey spectra were measured with pass energy of 187.850 eV and electronvolt step of 0.8 eV, while for the high-resolution spectra, pass energy of 23.500 eV and electronvolt step of 0.2 eV were used. The spectra were evaluated with the MultiPak (Ulvac - PHI, Inc.) software. All binding energy (BE) values were referenced to the carbon peak C 1s at 284.80 eV. The conversion and selectivity of the reactions were analyzed by GC employing chromatograph Agilent 6820 (Agilent, United States), equipped with flame ionization detector (FID) and chromatographic column DB5 (30×0.250×0.25). The following experimental parameters were applied: initial temperature 100 °C, increased to 250 °C with a rate of 10 °C/min. For ICP-MS analysis, samples were dissolved in a mixture of concentrated HNO_3 and HCl (both Analpure, Analytika, spol. s r.o., Czech Republic) and filled up to defined volume with ultra-pure water. All elements were quantified by ICP-MS (Agilent 7700x, Agilent, Japan) using external calibration and appropriate isotopes. The Raman spectrum of respective sample was collected through instrument, DXR Raman (Thermo, USA); laser wavelength: 633 nm, laser power on sample: 2 mW, exposition time: 5 s, 32 spectra were averaged at each spot to obtain one data point. Low pressure volumetric nitrogen adsorption–desorption measurements were performed at 77 K maintained by low temperature liquid nitrogen bath, with pressure ranging from 0 to 760 torr using an Autosorb iQ (Quantachrome Inc., USA) gas sorption system. Outgassing process was carried out at 200 °C for 15 h under dynamic vacuum (10^{-3} torr) until a constant weight was achieved. Ultrahigh purity grade (99.999%) N_2 was used, which is further purified by using calcium aluminosilicate adsorbents to remove trace amounts of water and other impurities prior to the measurements. For N_2 isotherms, warm and cold free-space correction measurements were performed with ultrahigh pure helium gas (99.999% purity). For the measurement, about 200 mg of samples were used and to confirm complete removal of all guest H_2O molecules from the samples, weight of the samples was measured before and after outgassing. Specific surface area was calculated by Brunauer–Emmett–Teller (BET) method obtained by using the data points (P/P_0 = 0.02 to 0.3) on the adsorption branch.

EPR measurements:

EPR measurements and analysis. EPR spectra were recorded on JEOL JES-X-320 operating at X-band frequency (~9.16–.17 GHz), equipped with a variable temperature control ES 13060DVT5 apparatus. The cavity Q quality factor was kept above 6000 in all measurements and signal saturation was avoided by working at low applied microwave power. Highly pure quartz tubes were employed (Suprasil, Wilmad, ≤0.5 OD). The spin trapping experiments were carried out as follows; the α-(4-pyridyl-1-oxide)-N-*tert*-butylnitrone (POBN) was initially dissolved in MeOH (10 mg/mL) and 0.2 mL of this solution was added to the reaction mixture containing 0.5 mmol (2 mL) of benzyl alcohol, 40 mg of catalyst, and a total of 2 mL of MeOH. The mixture was heated to 60 °C in air under stirring for 30 min, after that the mixture was centrifuged at 6000 rpm (5 min), and the supernatant collected for the EPR measurements (Fig. S13). Blank sample used for the EPR experiment was prepared as reported above, with the exception that the catalysts was not present and no EPR signal was observed. Additional experiment aimed to probe the effect on the radicals' formation, when MeOH was not added, was carried as follow; solid (10 mg) α-(4-pyridyl-1-oxide)-N-*tert*-butylnitrone (POBN) was added to the reaction mixture containing 2 mL of benzyl alcohol and 40 mg of catalyst. The mixture was heated to 60 °C in air under stirring for 30 min, after that the suspension was centrifuged at 6000 rpm (5 min), and the supernatant was collected for the EPR measurements. This experiment gave negative results (no radical species detected by X-band EPR on the fluid solution, Fig. S15). The experiment aimed to probe the effect on the radicals' formation in the presence of a limited amount of

MeOH was carried as follows: solid (10 mg) α-(4-pyridyl-1-oxide)-N-*tert*-butylnitrone (POBN) was added to the reaction mixture containing 2 mL of benzyl alcohol, 40 mg of catalyst, and 20 μL of MeOH. The mixture was heated to 60 °C in air under stirring for 30 min, after that the suspension was centrifuged at 6000 rpm (5 min), and the supernatant was collected for the EPR measurements (Fig. S14).

EPR analysis and theoretical modelling. Simulation of the EPR trace was carried out with the WinEPR SimFonia software (V.1.25, *EPR Division*, Bruker Instruments, Inc., Billerica, USA) using second-order perturbation theory, according to the following spin-Hamiltonian:

Solution spectra: $H = g\ \mu_B\ B_0\ S + a\ S.I + g_n\ \mu_N\ B_0\ I$

The theoretical modeling and geometry optimization of the POBN radical species (POBN-CH_2OH and POBN-H) were performed by density functional theory (DFT) in the gas phase (neutral charge) using an unrestricted BP86 functional with the Euler–Maclaurin–Lebedev grid (70, 302) and basis set 6-31G* for all atoms, as implemented in the computational package Spartan 10 (Ver. 1.1.0, Wavefunction Inc., Irvine, CA 92612). The SCF convergence and gradient convergence were set to 10^{-7} a.u. for the energy change and <0.0003, respectively. The coordinate file (TRIPOS, mol2) for POBN-CH_2OH is given in Table S3 material and for POBN-H in Table S5. Fermi contact terms were calculated with Gaussian09 program[1] (DFT/UB3LYP/6-31G*(d,p), vacuum, S = 1/2, neutral molecule) and are given for POBN-CH_2OH in Table S4 and for POBN-H in Table S6.

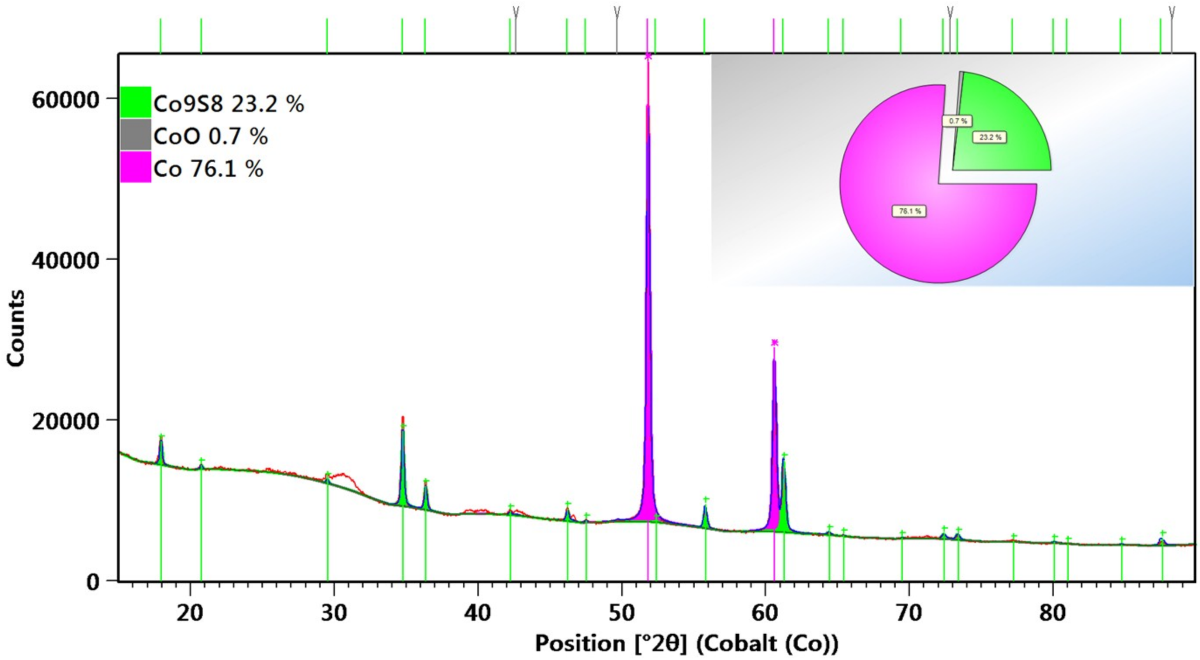

Fig. S1 Result of the Rietveld refinement of sample Co@NOSC, showing the Co, Co_9S_8 and CoO crystalline phases.

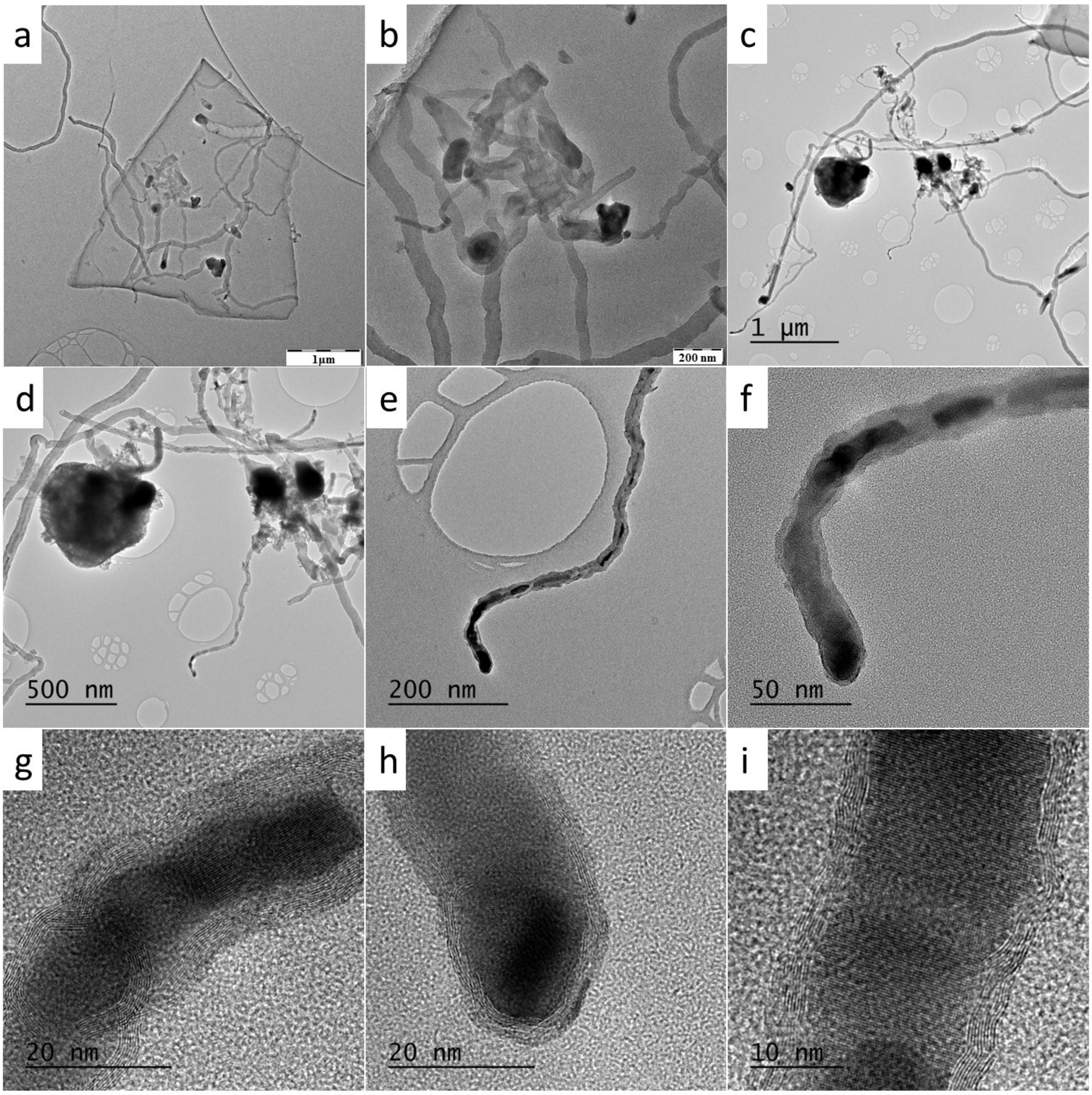

Fig. S2 (a), (b) are TEM and (c) to (i) are the HRTEM images of Co@NOSC catalyst.

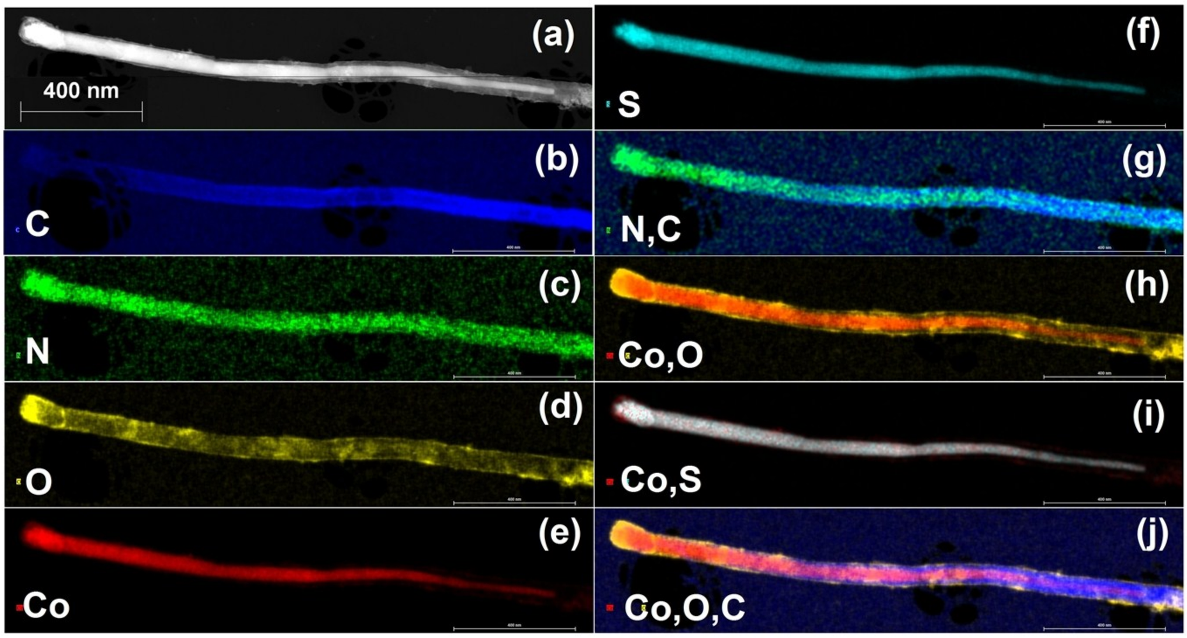

Fig. S3 STEM elemental mapping images of Co@NOSC catalyst (a), HAADF image (b–j) for different elements at 400 nm scale bar.

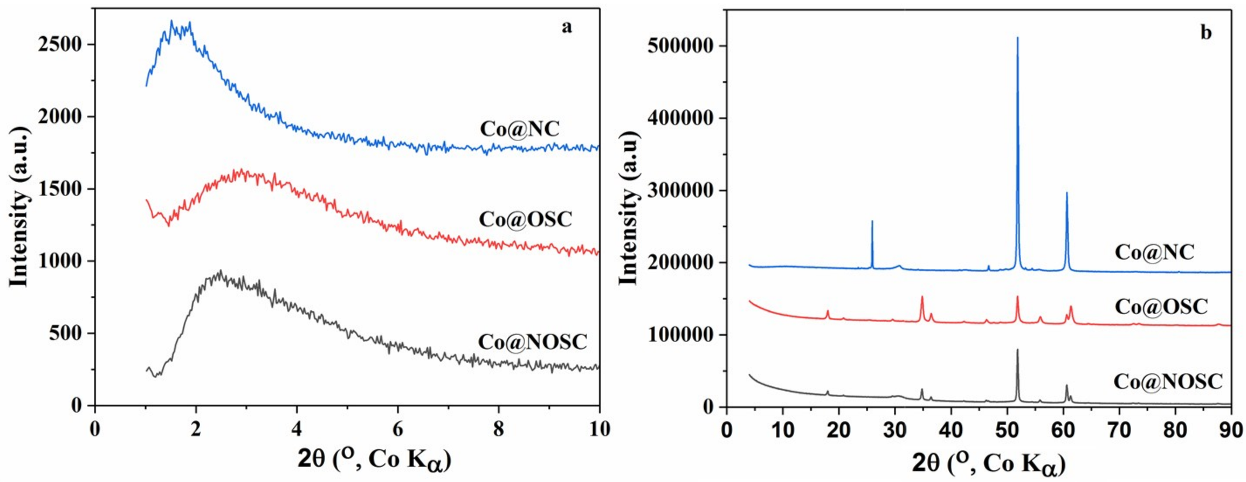

Fig. S4 (a) Low angle XRD pattern of synthesized samples Co@NOSC, Co@OSC, and Co@NC catalyst. (b) Wide angle XRD pattern of corresponding samples.

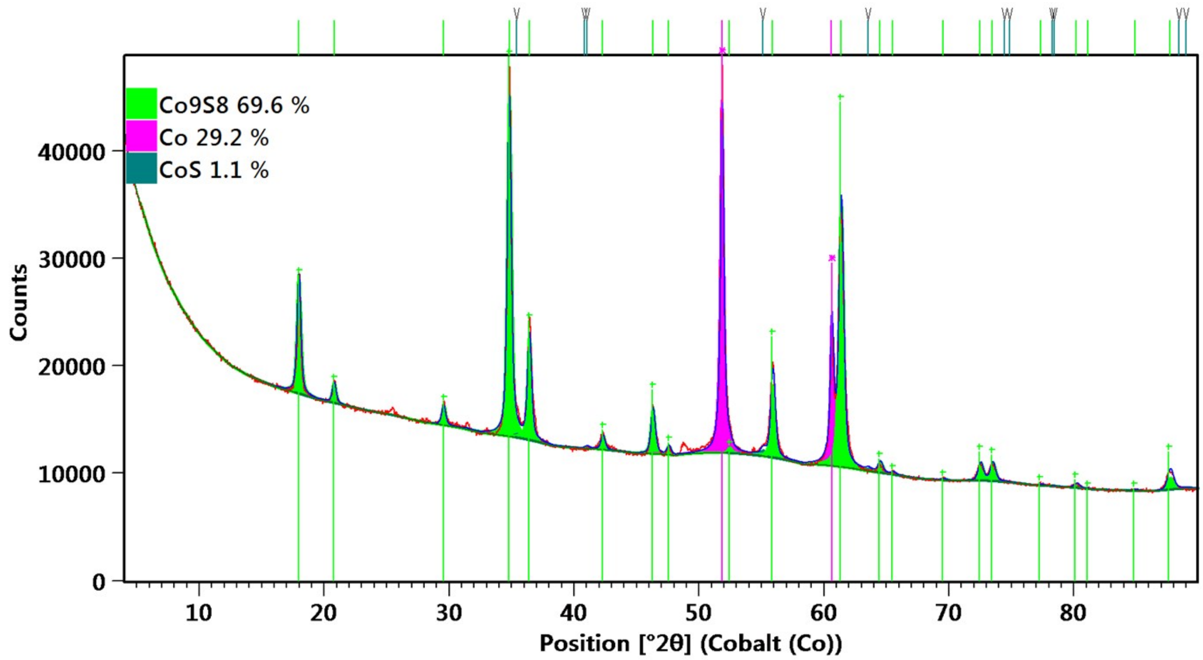

Fig. S5 Result of the Rietveld refinement of sample Co@OSC, showing the Co, Co_9S_8 and CoS crystalline phases.

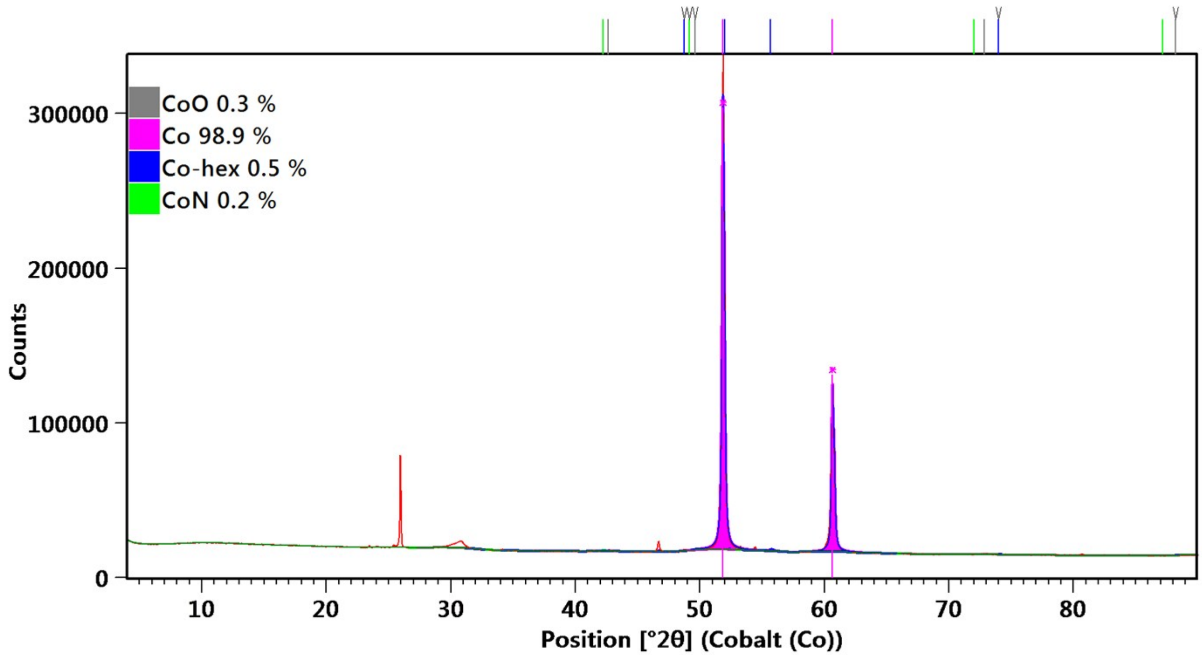

Fig. S6 Result of the Rietveld refinement of sample Co@NC, showing the CoO, Co, Co-hex and CoN crystalline phases.

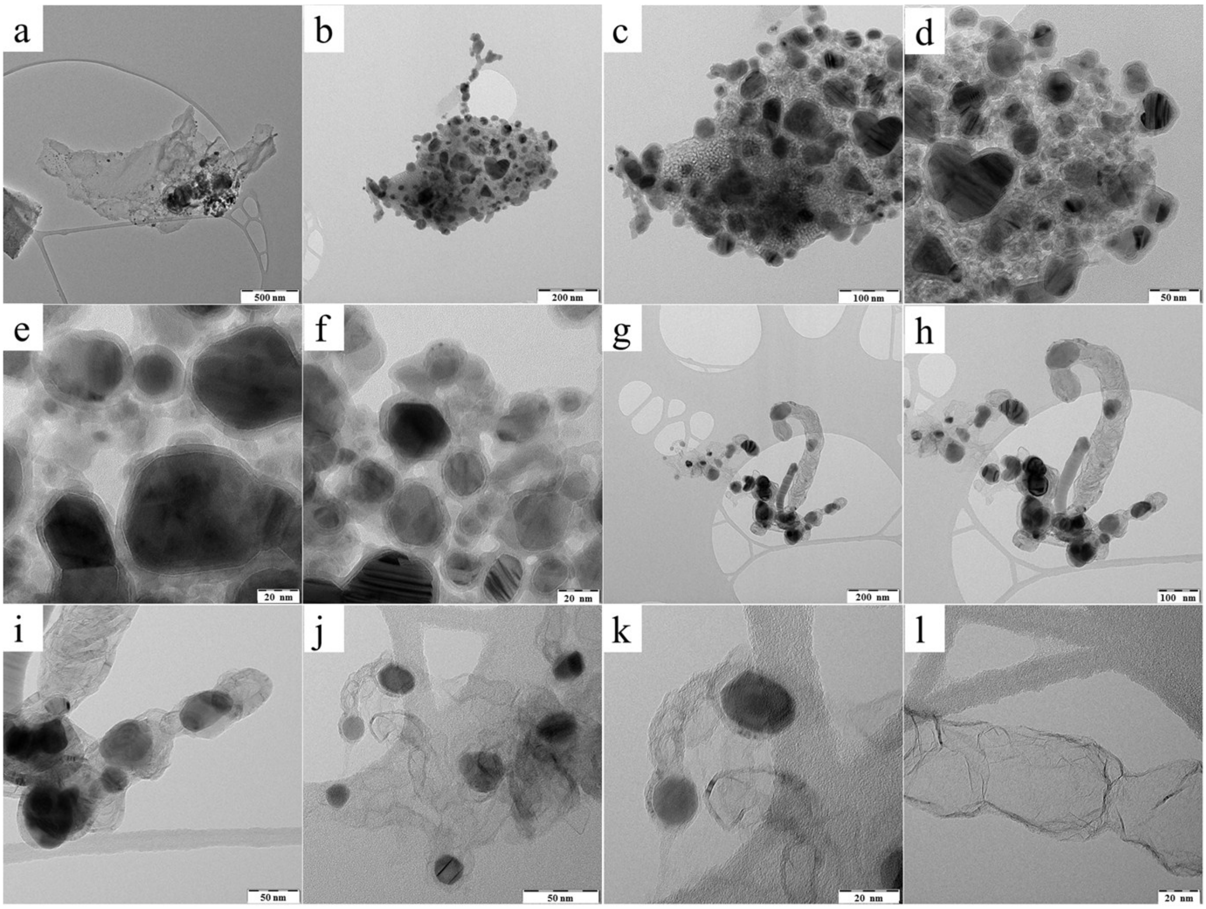

Fig. S7 TEM images (a), to (f) of Co@OSC and (g), to (l) of Co@NC materials.

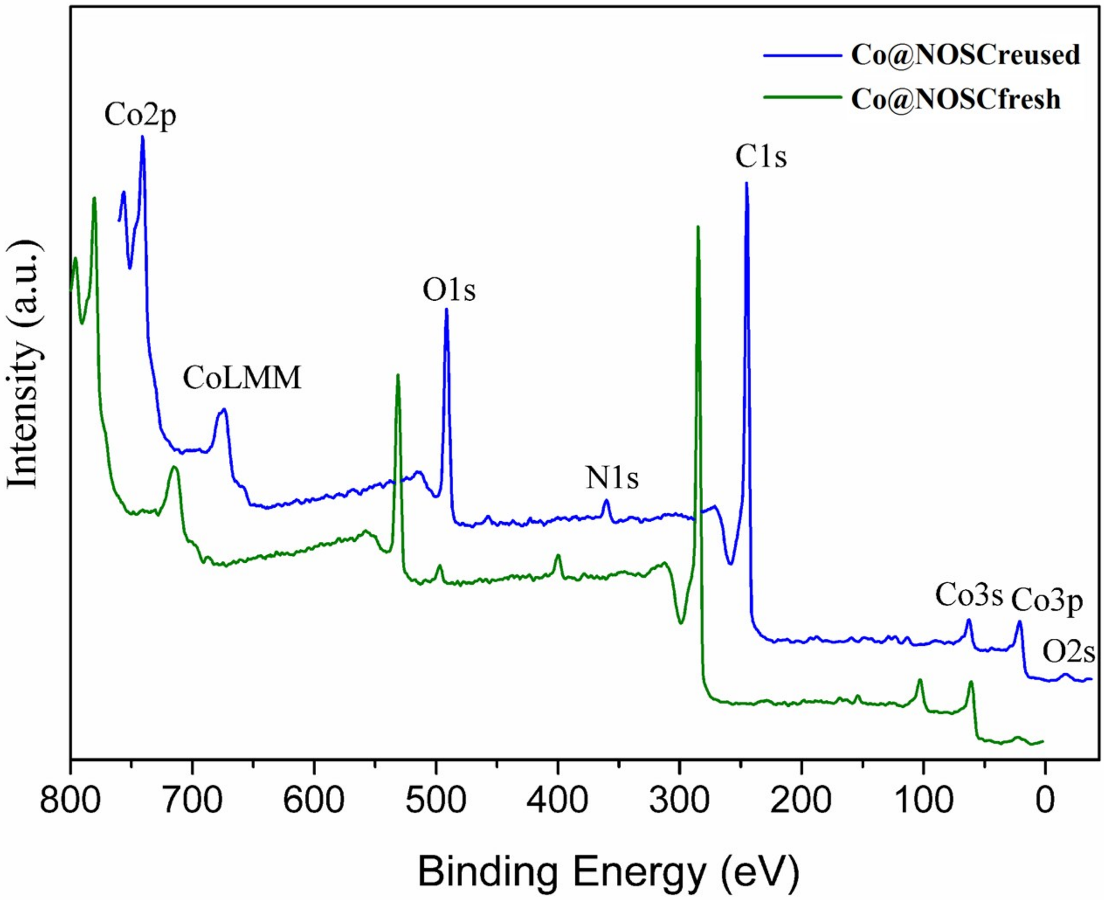

Fig. S8 XPS survey scan of fresh and reused Co@NOSC catalyst.

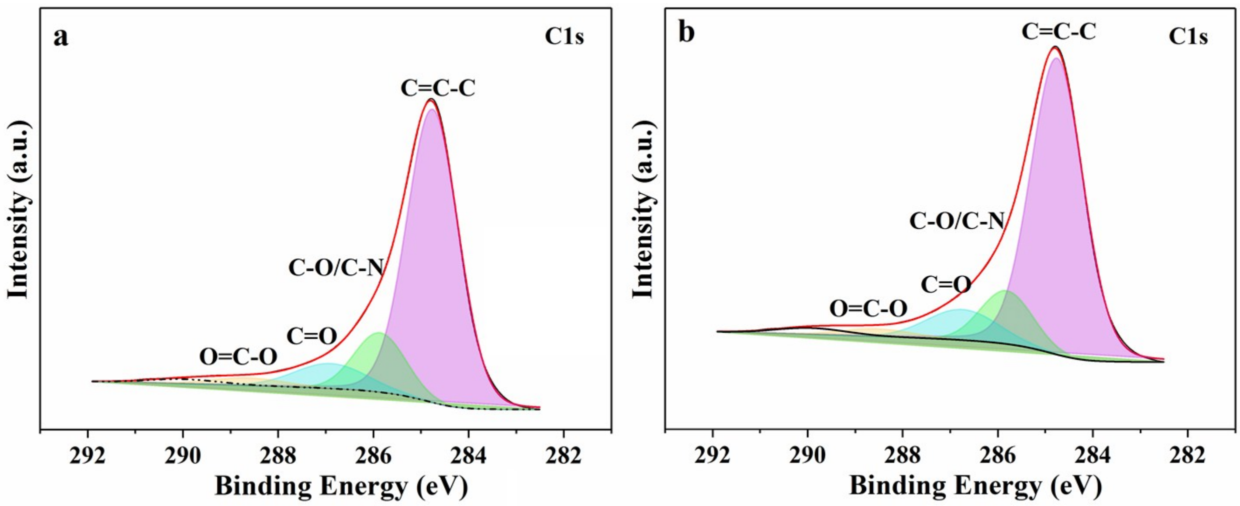

Fig. S9 The HR-XPS of C1s fresh (a) and reused (b) catalyst.

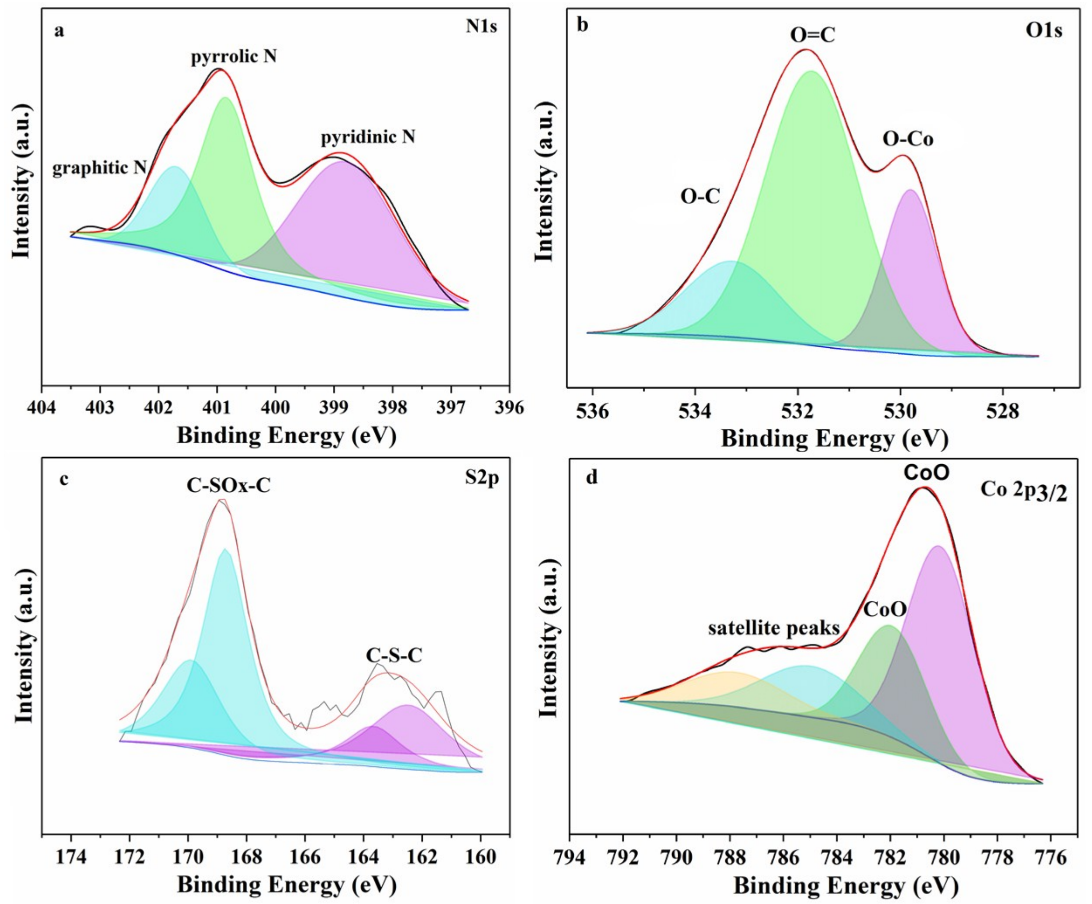

Fig. S10 XPS spectra of Co@NOSC catalyst (after reaction). (a) N1s, (b) O1s, (c) S2p, and (d) Co2p region.

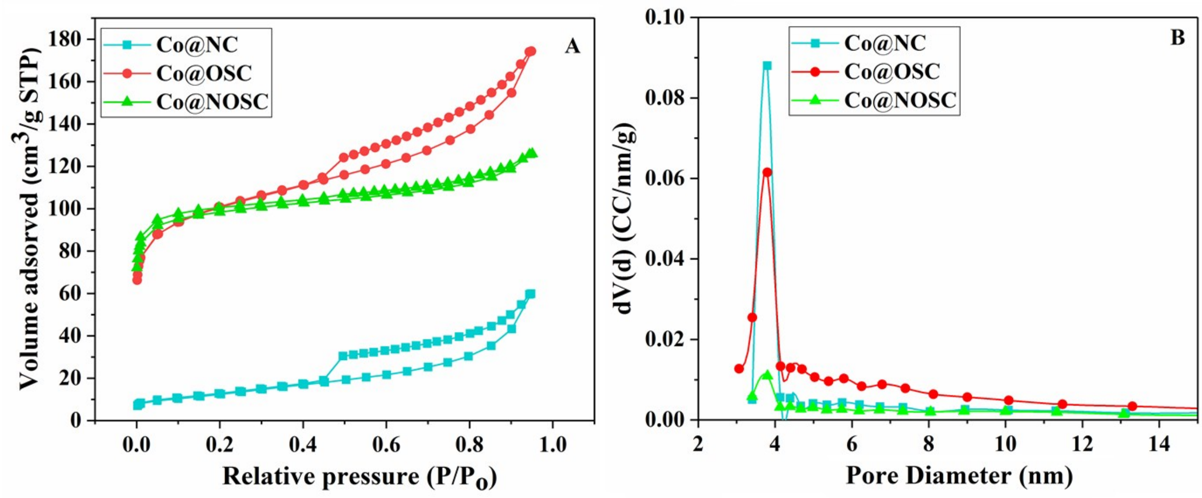

Fig. S11 (A) N_2 adsorption and desorption isotherm Co@NC, Co@OSC and Co@NOSC (B) Respective BJH pore size distribution.

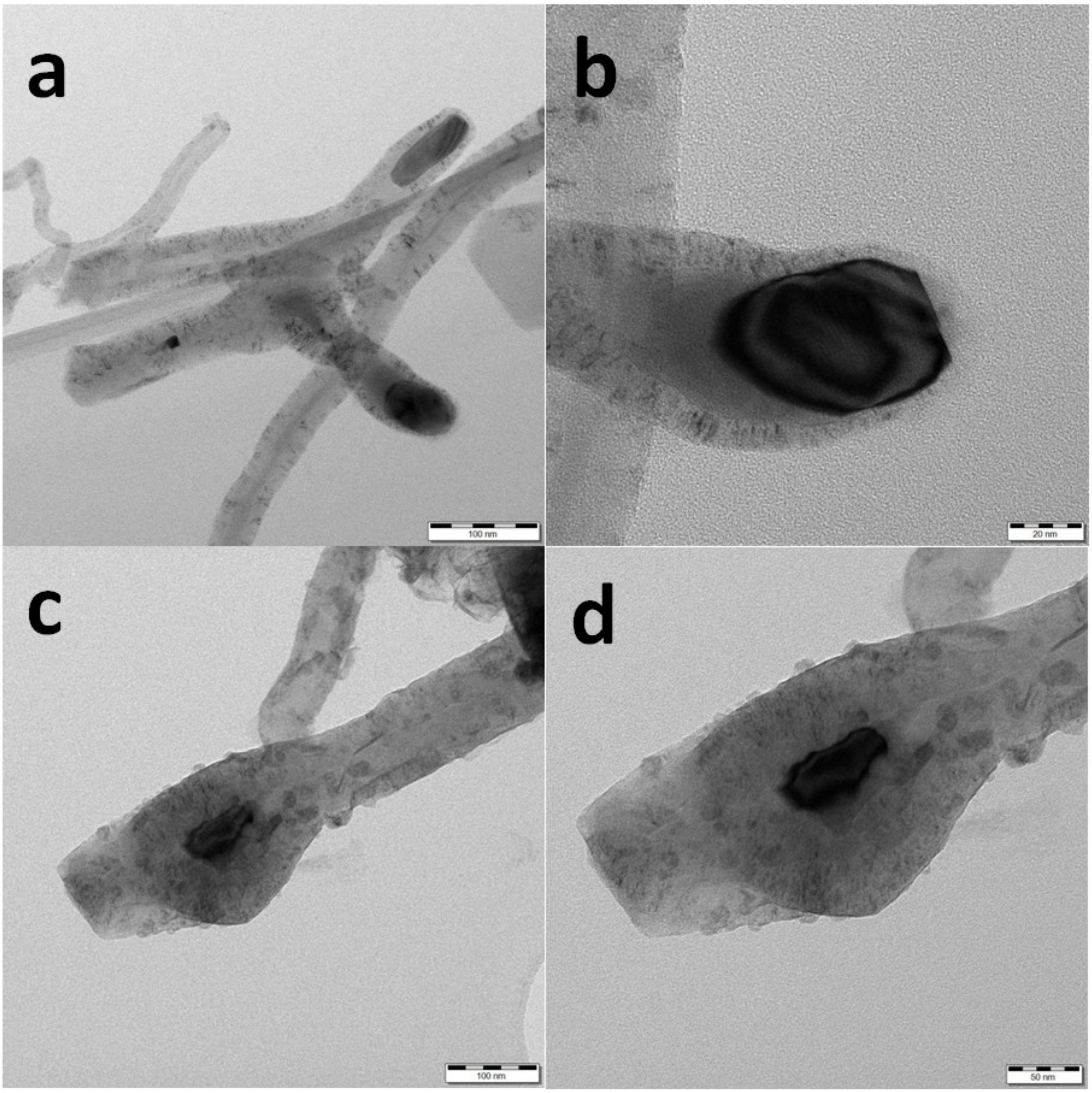

Fig. S12 TEM images of (a,b) fresh Co@NOSC and (c,d) reused Co@NOSC after 6th cycle.

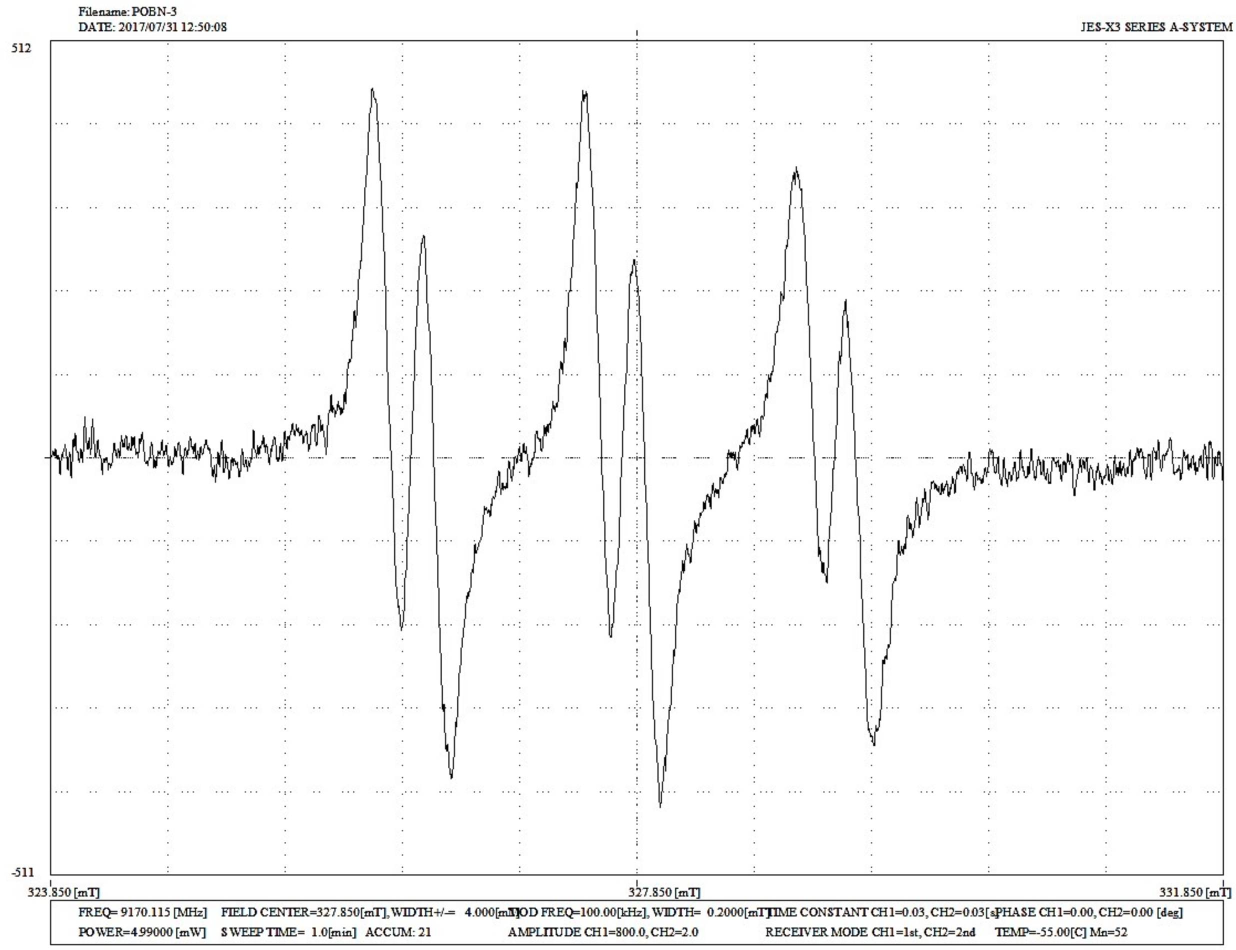

Fig. S13 X-band (9.17 GHz) EPR spectrum of the radical species collected from the catalyst/benzyl alcohol/POBN/MeOH mixture. Experimental parameters: frequency 9.170115 GHZ, 100 kHz modulation frequency, 0.2 mT modulation width, 0.03 s time constant, 4.9900 mW microwave power, sweep time of 1 min, 21 scans accumulated and averaged, T = 218 K.

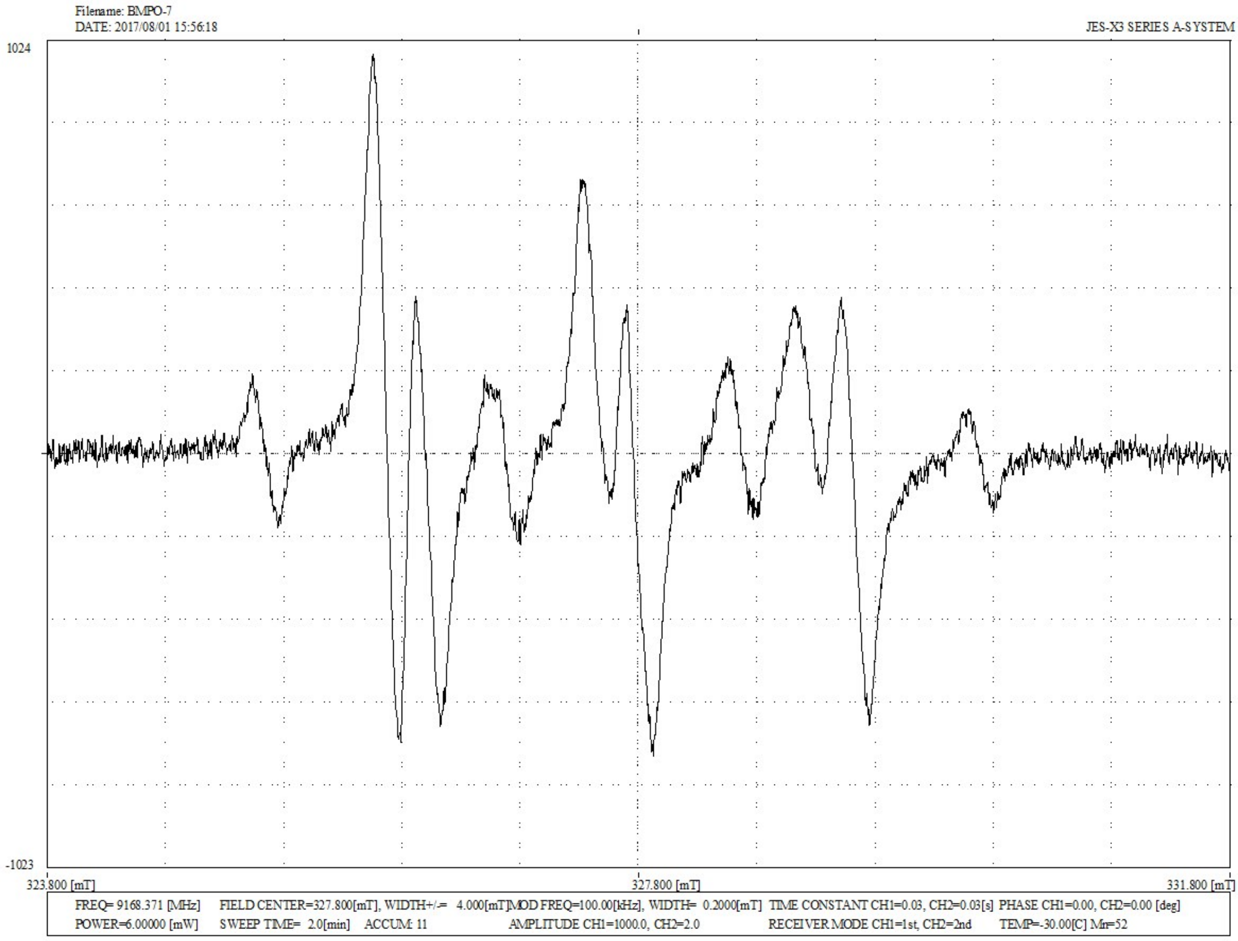

Fig. S14 X-band (9.17 GHz) EPR spectrum of the radical species collected from the catalyst/benzyl alcohol/POBN/MeOH mixture to which small amounts of MeOH were added (limited reactant, see Experimental section for details). Experimental parameters: frequency 9.168371 GHZ, 100 kHz modulation frequency, 0.2 mT modulation width, 0.03 s time constant, 6.000 mW microwave power, sweep time of 2 min, 11 scans accumulated and averaged, T = 243 K.

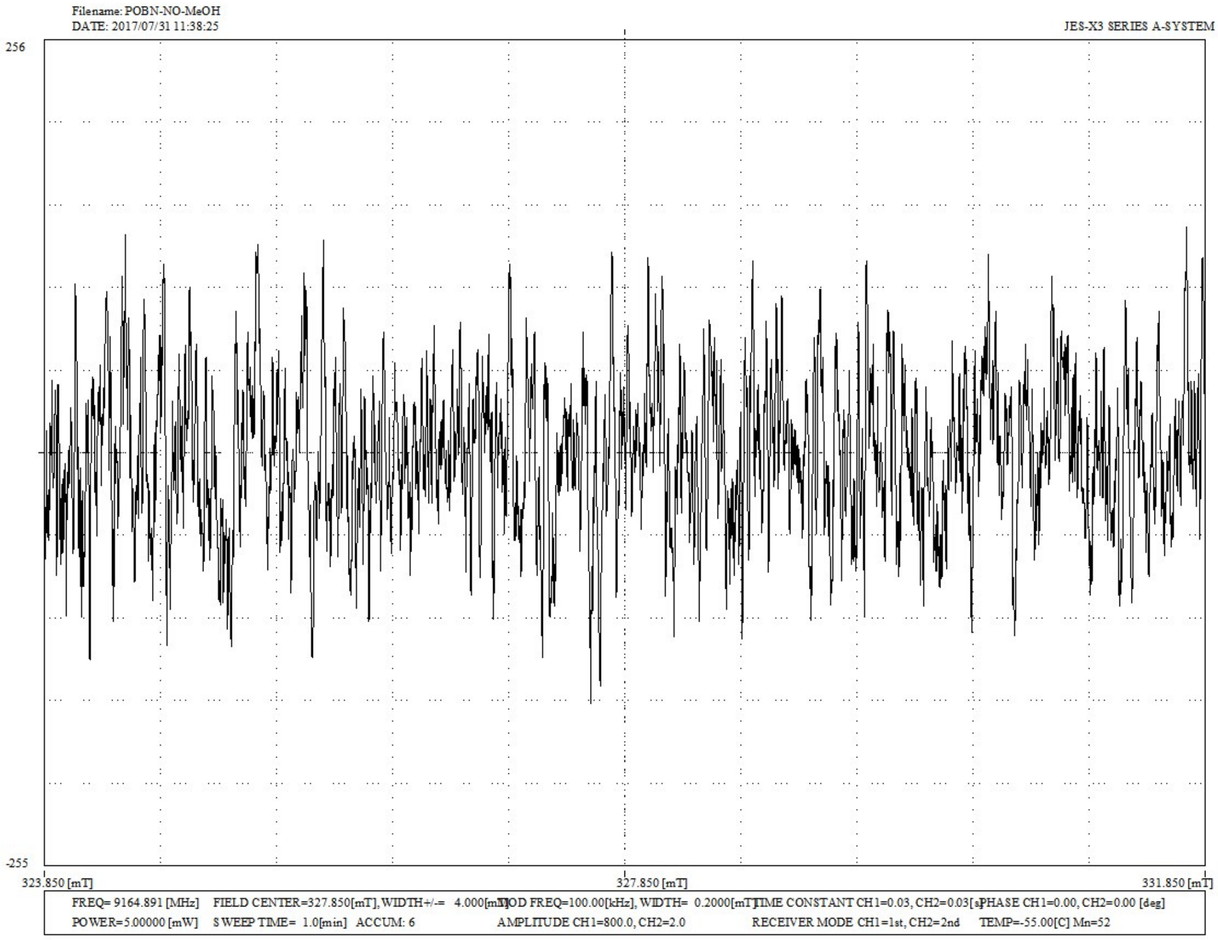

Fig. S15 X-band (9.16 GHz) EPR spectrum (T = 218 K) of the supernatant collected from the catalyst/benzyl alcohol/POBN mixture after centrifugation and without the presence of the MeOH solvent, indicating that MeOH is pivotal for trapping the radical species. Experimental parameters: frequency 9.164891 GHZ, 100 kHz modulation frequency, 0.2 mT modulation width, 0.03 s time constant, 5.000 mW microwave power, sweep time of 1 min, 6 scans accumulated and averaged, T = 218 K.

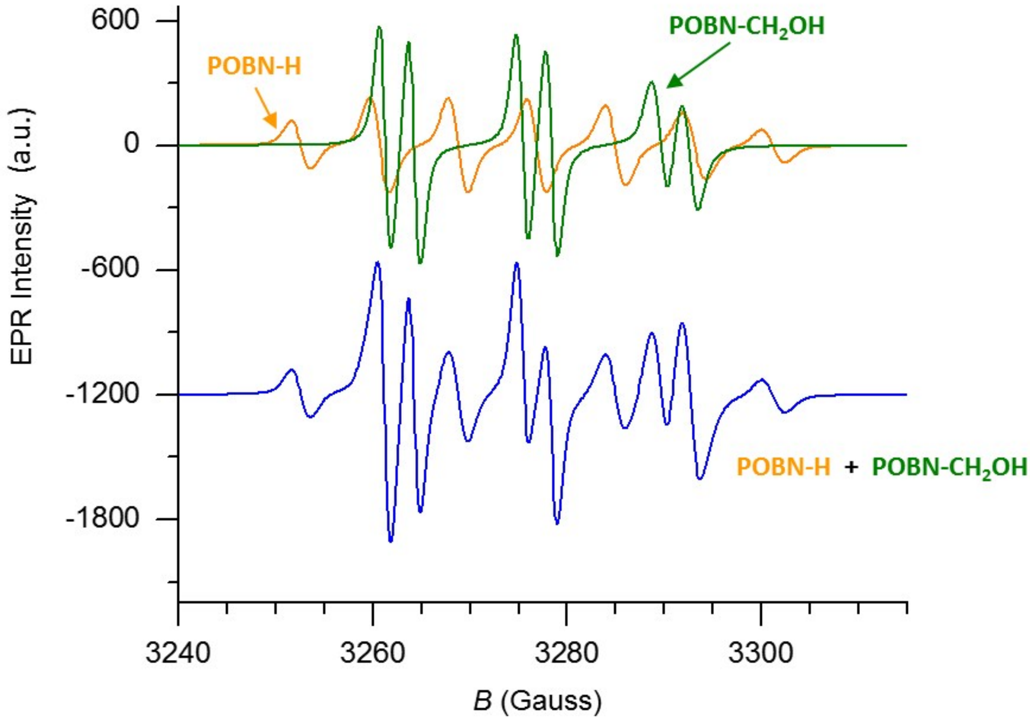

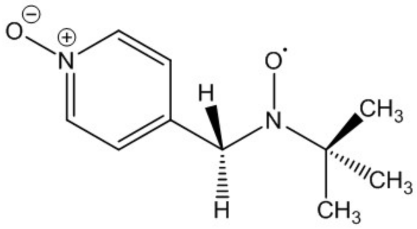

POBN-H
- 1N, (a_N) of 16.20 G,
- 2H, (a_H) of 8.10 G,
- Lorentzian/Gaussian ratio of 0.22
- line-width function (a+bm+cm^2)
- a = 1.99, b = -0.20 and c = 0.18
- g_{iso} = 2.0052

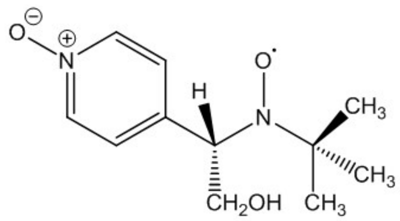

POBN-CH_2OH
- 1N (a_N) of 14.35 G, 1H (a_H) of 3.0 G,
- Lorentzian/Gaussian ratio of 0.23
- line-width function (a+bm+cm^2)
- a = 1.30, b = -0.25 and c = 0.20
- g_{iso} = 2.0052

Fig. S16 Simulation of the EPR resonance shown in Fig. S12 (catalyst/benzyl alcohol/POBN/MeOH mixture to which small amounts of MeOH was added) obtained by third-order perturbation theory (WinEPR SimFonia software, V. 1.25). The individual components are shown with orange (POBN-H) and green lines (POBN-CH_2OH). Their sum is shown by the blue trace. Parameters used in the spin-Hamiltonian simulations are given next to the molecule drawings.

Table S1: Textural properties of the synthesized materials.

Sample	SA_{BET} /m^2g^{-1a}	SAmi /m^2g^{-1b}	SAme /m^2g^{-1c}	Vmi /$cm^3\ g^{-1d}$	D /nm[e]
Co@NOSC	383.09	347.82	35.27	0.138	3.8
Co@OSC	369.90	274.80	95.10	0.116	3.8
Co@NC	45.90	0	45.90	0	3.8

[a]BET surface area. [b]Micropore surface area calculated from t-plot method. [c]Mesopore surface area calculated as SA_{BET}-SA_{mi}. [d]Micropore volume calculated from t-plot method. [e]BJH adsorption average pore diameter.

Table S2: Comparative performance of Co@NOSC catalyst with prior reported art.

Catalyst	Time (h)	Temp. (°C)	Base (mmol)	BA (mmol)	Conv./Yield (%)	Select. (%)	Ref.
Co@NC-4	12	60	-	0.5	99	98	2
Co@NC-4	1	60	0.1	0.5	89	98	2
Co_3O_4-N@C	24	80	0.1	0.5	97	-	3
Co_3O_4-Al_2O_3	24	60	0.1	0.5	83/79	-	3
Co_3O_4-TiO_2	24	60	0.1	0.5	52/45	-	3
Co-CoO@NC	24	80	0.2	1	100	100	4
Co@C-N[a]	96	25	-	0.5	99>	100	5
PdBiTe	8	60	25 mol %	1 mol	99>	100	6
$[PdCl_2(CH_3CN)_2]$	12	45	1	0.5	74	-	7
Au-Pd@HT-PO_4^{3-}	24	55	-	0.2	76	-	8
Co@NOSC	**24**	**60**	**Without base**	**0.5**	**97>**	**98>**	**Present work**

[a]Hexane was used as a solvent.

Table S3 The coordinate file (TRIPOS, mol2) for the POBN-CH_2OH radical adduct obtained from optimized geometry (vacuum) calculated by DFT/UPB86/6-31G*.

```
#
#        File Created by: Spartan '10 Export
#

@<TRIPOS>MOLECULE
M0001
33 33
SMALL
MULLIKEN_CHARGES


@<TRIPOS>ATOM
    1   N1       -1.196805066    0.663117670    0.329319859    N.3   1  M0001   -0.013996
    2   C2       -2.023093575   -0.567180960    0.029210545    C.3   1  M0001    0.176717
    3   C3       -1.614952134   -1.677843491    1.024067754    C.3   1  M0001   -0.480019
    4   H4       -1.709558384   -1.303267389    2.056521236      H   1  M0001    0.181682
    5   H5       -0.572049173   -1.998521988    0.857559541      H   1  M0001    0.166899
    6   H6       -2.273720132   -2.555862125    0.903198774      H   1  M0001    0.156905
    7   C7       -1.812678627   -1.036871778   -1.419898806    C.3   1  M0001   -0.513292
    8   H8       -0.769919721   -1.345368567   -1.611173622      H   1  M0001    0.170390
    9   H9       -2.099906280   -0.261024106   -2.152137789      H   1  M0001    0.167136
   10   H10      -2.454554244   -1.916365673   -1.603383251      H   1  M0001    0.171769
   11   C11      -3.496457816   -0.166808192    0.255222591    C.3   1  M0001   -0.474862
   12   H12      -3.620868079    0.249491872    1.267520990      H   1  M0001    0.188338
   13   H13      -4.148145189   -1.051196344    0.148078774      H   1  M0001    0.155750
   14   H14      -3.814924873    0.594216026   -0.479070540      H   1  M0001    0.157240
   15   O15      -1.306847601    1.166704856    1.519006043      O   1  M0001   -0.386625
   16   C16      -0.023921838    1.093664152   -0.465410101    C.3   1  M0001   -0.107896
   17   C17       1.250128195    0.347348618   -0.090196470   C.ar   1  M0001    0.188702
   18   N18       3.682995802   -0.955672381    0.601336895  N.pl3   1  M0001   -0.005501
   19   C19       1.570535349    0.042346184    1.249340223   C.ar   1  M0001   -0.234663
   20   C20       2.196623462   -0.019634760   -1.066491806   C.ar   1  M0001   -0.222255
   21   C21       3.382121588   -0.655095405   -0.718496385   C.ar   1  M0001    0.049572
   22   C22       2.757843406   -0.599136792    1.573265272   C.ar   1  M0001    0.050196
   23   H23       0.871780913    0.304169530    2.050977884      H   1  M0001    0.187264
   24   H24       2.021380769    0.206208199   -2.123757717      H   1  M0001    0.164412
   25   H25       4.158204561   -0.962982947   -1.420866446      H   1  M0001    0.185825
   26   H26       3.067717771   -0.870195117    2.583737109      H   1  M0001    0.187318
   27   O27       4.775479552   -1.544258210    0.913645948      O   1  M0001   -0.481147
   28   H28      -0.245244138    0.905054891   -1.529322729      H   1  M0001    0.170491
   29   C29       0.135428434    2.624867528   -0.316904776    C.3   1  M0001   -0.076598
   30   H30       0.491657002    2.859764797    0.703168862      H   1  M0001    0.163996
   31   H31      -0.857695845    3.102580144   -0.455102588      H   1  M0001    0.150017
   32   O32       1.065583839    3.023552675   -1.328006333    O.3   1  M0001   -0.594101
   33   H33       1.408968156    3.902787101   -1.074452698      H   1  M0001    0.400338

@<TRIPOS>BOND
    1       1      2     1
    2       3      4     1
    3       3      5     1
    4       3      6     1
    5       2      3     1
    6       7      8     1
    7       7      9     1
    8       7     10     1
    9       2      7     1
   10      11     12     1
   11      11     13     1
   12      11     14     1
   13       2     11     1
   14       1     15     1
   15       1     16     1
   16      17     20     ar
   17      20     21     ar
   18      18     21     ar
   19      18     22     ar
   20      19     22     ar
   21      17     19     ar
   22      21     25     1
   23      22     26     1
   24      19     23     1
   25      20     24     1
   26      16     17     1
   27      27     18     1
   28      16     28     1
   29      29     30     1
   30      29     31     1
   31      16     29     1
   32      32     33     1
   33      29     32     1
```

Table S4 Calculated Fermi contact couplings for the POBN-CH_2OH radical adduct (DFT/UB3LYP/6-31G*(d,p), vacuum, neutral molecule). The atomic numbering is given in the molecule drawing.

```
# ub3lyp/6-31+g(d,p) scf=qc geom=connectivity
```

	Atom	a.u.	MegaHertz	Gauss	$10^{(-4)}$ cm^{-1}
1	**N(14)**	**0.11331**	**36.60944**	**13.06316**	**12.21159**
2	C(13)	-0.00950	-10.67505	-3.80912	-3.56081
3	C(13)	0.01191	13.38664	4.77668	4.46530
4	H(1)	-0.00052	-2.33417	-0.83289	-0.77860
5	H(1)	-0.00039	-1.72753	-0.61643	-0.57624
6	H(1)	0.00056	2.49187	0.88916	0.83120
7	C(13)	-0.00017	-0.19569	-0.06983	-0.06527
8	H(1)	-0.00011	-0.50745	-0.18107	-0.16927
9	H(1)	-0.00007	-0.30032	-0.10716	-0.10018
10	H(1)	-0.00040	-1.78502	-0.63694	-0.59542
11	C(13)	0.00973	10.93713	3.90264	3.64823
12	H(1)	-0.00032	-1.43386	-0.51164	-0.47828
13	H(1)	-0.00009	-0.38070	-0.13584	-0.12699
14	H(1)	-0.00027	-1.22839	-0.43832	-0.40975
15	O(17)	0.08327	-50.47559	-18.01094	-16.83684
16	C(13)	-0.00906	-10.18901	-3.63569	-3.39869
17	C(13)	0.02859	32.14266	11.46930	10.72164
18	N(14)	0.00029	0.09379	0.03347	0.03128
19	C(13)	0.00111	1.25173	0.44665	0.41753
20	C(13)	0.00273	3.07027	1.09555	1.02413
21	C(13)	0.00048	0.53884	0.19227	0.17974
22	C(13)	0.00088	0.98733	0.35230	0.32934
23	H(1)	0.00022	0.97277	0.34711	0.32448
24	H(1)	-0.00005	-0.21618	-0.07714	-0.07211
25	H(1)	0.00021	0.91646	0.32702	0.30570
26	H(1)	0.00002	0.10034	0.03580	0.03347
27	O(17)	0.00098	-0.59296	-0.21158	-0.19779
28	**H(1)**	**0.00179**	**8.01692**	**2.86064**	**2.67416**
29	C(13)	0.00563	6.32744	2.25779	2.11061
30	H(1)	-0.00004	-0.18632	-0.06648	-0.06215
31	H(1)	-0.00016	-0.72646	-0.25922	-0.24232
32	O(17)	0.00044	-0.26903	-0.09600	-0.08974
33	H(1)	0.00022	0.99212	0.35401	0.33094

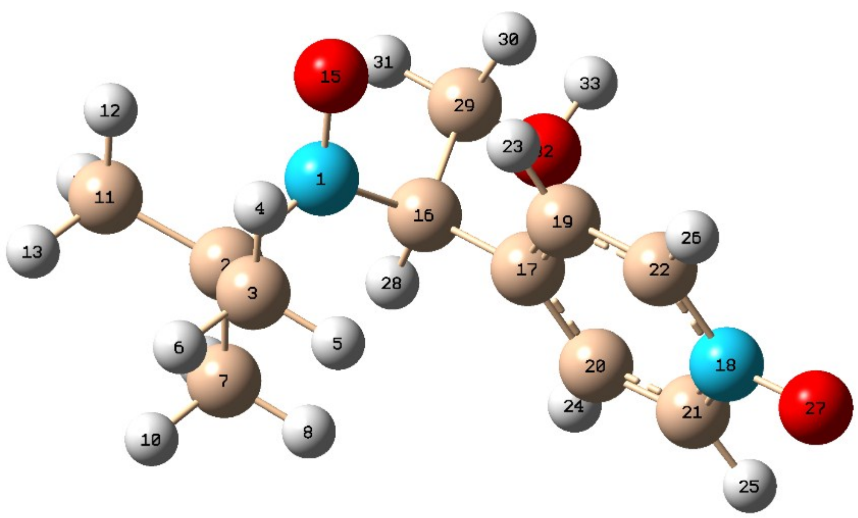

Table S5 The coordinate file (TRIPOS, mol2) for the POBN-H radical adduct obtained from optimized geometry (vacuum) calculated by DFT/UPB86/6-31G*.

```
#       File Created by: Spartan '10 Export
#

@<TRIPOS>MOLECULE
M0001
29 29
SMALL
MULLIKEN_CHARGES


@<TRIPOS>ATOM
    1    N1     -0.909818638    0.365365347    0.816897585    N.3   1  M0001   0.026240
    2    C2     -2.002536746   -0.233409522   -0.015216552    C.3   1  M0001   0.152101
    3    C3     -2.645374182   -1.362479121    0.800567548    C.3   1  M0001  -0.476759
    4    H4     -3.068626545   -0.985014473    1.732788956      H   1  M0001   0.186831
    5    H5     -1.907789190   -2.131216500    1.050520693      H   1  M0001   0.170762
    6    H6     -3.442244317   -1.823759483    0.207702953      H   1  M0001   0.152588
    7    C7     -1.402768101   -0.805380355   -1.312005074    C.3   1  M0001  -0.491289
    8    H8     -0.626841844   -1.545084489   -1.091189097      H   1  M0001   0.179381
    9    H9     -0.967826781   -0.031040932   -1.952563611      H   1  M0001   0.154452
   10    H10    -2.191830177   -1.298421097   -1.889751860      H   1  M0001   0.168861
   11    C11    -3.044465799    0.860832729   -0.325785298    C.3   1  M0001  -0.479239
   12    H12    -3.448414742    1.274936836    0.603639527      H   1  M0001   0.179973
   13    H13    -3.873587790    0.442229099   -0.907287735      H   1  M0001   0.165358
   14    H14    -2.610011683    1.680704078   -0.909642841      H   1  M0001   0.155942
   15    O15    -0.977181275    0.302354503    2.098566386      O   1  M0001  -0.394942
   16    C16     0.087755530    1.296287626    0.264827745    C.3   1  M0001  -0.273364
   17    C17     1.468148939    0.680792638    0.157473666   C.ar   1  M0001   0.186155
   18    N18     4.058383203   -0.427250363   -0.014913768  N.pl3   1  M0001  -0.002083
   19    C19     2.040044125   -0.018830924    1.229885778   C.ar   1  M0001  -0.224807
   20    C20     2.242946326    0.801453620   -0.999180342   C.ar   1  M0001  -0.241019
   21    C21     3.512515167    0.255512748   -1.072070447   C.ar   1  M0001   0.059029
   22    C22     3.306239309   -0.558101133    1.129785241   C.ar   1  M0001   0.057110
   23    H23     1.481833145   -0.151075800    2.150886551      H   1  M0001   0.188895
   24    H24     1.865474260    1.329061019   -1.871194351      H   1  M0001   0.150720
   25    H25     4.161814034    0.311588817   -1.935273581      H   1  M0001   0.185468
   26    H26     3.807196253   -1.109520638    1.914087674      H   1  M0001   0.188791
   27    O27     5.227906070   -0.928771007   -0.089940753      O   1  M0001  -0.486180
   28    H28    -0.241878449    1.651560524   -0.715519249      H   1  M0001   0.162710
   29    H29     0.100939841    2.156676201    0.943904308      H   1  M0001   0.198316

@<TRIPOS>BOND
    1     1     2    1
    2     3     4    1
    3     3     5    1
    4     3     6    1
    5     2     3    1
    6     7     8    1
    7     7     9    1
    8     7    10    1
    9     2     7    1
   10    11    12    1
   11    11    13    1
   12    11    14    1
   13     2    11    1
   14     1    15    1
   15     1    16    1
   16    17    20    ar
   17    20    21    ar
   18    18    21    ar
   19    18    22    ar
   20    19    22    ar
   21    17    19    ar
   22    21    25    1
   23    22    26    1
   24    19    23    1
   25    20    24    1
   26    16    17    1
   27    27    18    1
   28    16    28    1
   29    16    29    1
```

Table S6 Calculated Fermi contact couplings for the POBN-H radical adduct (DFT/UB3LYP/6-31G*(d,p), vacuum, neutral molecule). The atomic numbering is given in the molecule drawing.

```
 ------------------------------------
 # b3lyp/6-31+g(d,p) geom=connectivity
 ------------------------------------
```

Isotropic Fermi Contact Couplings

	Atom	a.u.	MegaHertz	Gauss	$10^{(-4)}$ cm^{-1}
1	**N(14)**	0.10637	34.36732	**12.26311**	11.46370
2	C(13)	-0.01006	-11.30654	-4.03446	-3.77146
3	C(13)	0.00250	2.80519	1.00096	0.93571
4	H(1)	-0.00013	-0.59354	-0.21179	-0.19798
5	H(1)	0.00006	0.26271	0.09374	0.08763
6	H(1)	-0.00039	-1.73613	-0.61949	-0.57911
7	C(13)	0.01068	12.00478	4.28360	4.00436
8	H(1)	-0.00018	-0.82456	-0.29422	-0.27504
9	H(1)	-0.00014	-0.60494	-0.21586	-0.20179
10	H(1)	0.00039	1.74616	0.62307	0.58246
11	C(13)	0.02050	23.04090	8.22156	7.68562
12	H(1)	-0.00049	-2.18584	-0.77996	-0.72912
13	H(1)	0.00188	8.39575	2.99581	2.80052
14	H(1)	-0.00026	-1.17842	-0.42049	-0.39308
15	O(17)	0.08104	-49.12347	-17.52848	-16.38583
16	C(13)	-0.01191	-13.39457	-4.77951	-4.46795
17	C(13)	0.02401	26.99575	9.63275	9.00481
18	N(14)	0.00007	0.02125	0.00758	0.00709
19	C(13)	-0.00019	-0.21857	-0.07799	-0.07291
20	C(13)	0.00017	0.19654	0.07013	0.06556
21	C(13)	0.00023	0.25393	0.09061	0.08470
22	C(13)	0.00073	0.81883	0.29218	0.27313
23	H(1)	0.00012	0.53989	0.19265	0.18009
24	H(1)	-0.00004	-0.15811	-0.05642	-0.05274
25	H(1)	0.00010	0.42900	0.15308	0.14310
26	H(1)	0.00000	0.01892	0.00675	0.00631
27	O(17)	0.00043	-0.26024	-0.09286	-0.08681
28	**H(1)**	0.00201	8.96443	**3.19873**	2.99021
29	**H(1)**	0.00550	24.57232	**8.76802**	8.19645

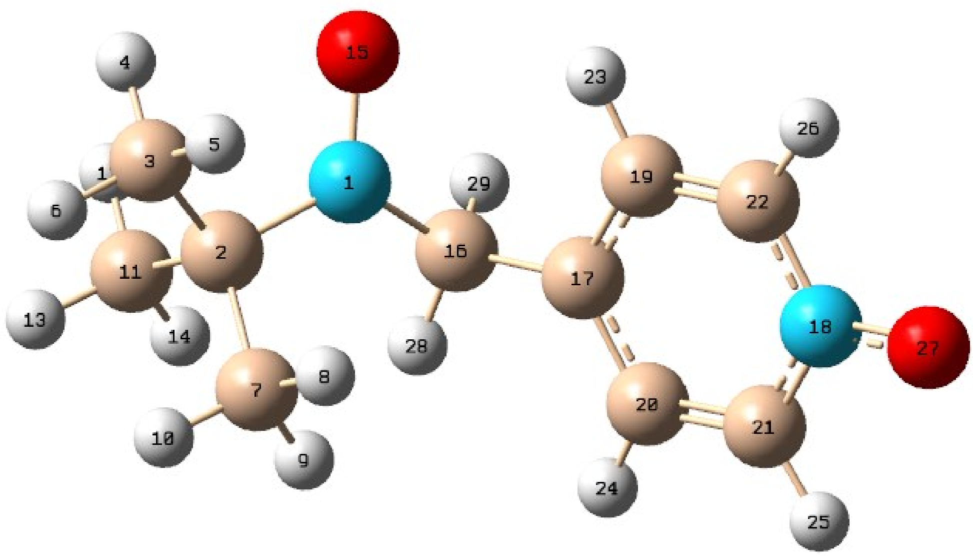

References

1 M. J. Frisch, G. W. Trucks, H. B. Schlegel, G. E. Scuseria, M. A. Robb, J. R. Cheeseman, G. Scalmani, V. Barone, G. A. Petersson, H. Nakatsuji, X. Li, M. Caricato, A. Marenich, J. Bloino, B. G. Janesko, R. Gomperts, B. Mennucci, H. P. Hratchian, J. V. Ortiz, A. F. Izmaylov, J. L. Sonnenberg, D. Williams-Young, F. Ding, F. Lipparini, F. Egidi, J. Goings, B. Peng, A. Petrone, T. Henderson, D. Ranasinghe, V. G. Zakrzewski, J. Gao, N. Rega, G. Zheng, W. Liang, M. Hada, M. Ehara, K. Toyota, R. Fukuda, J. Hasegawa, M. Ishida, T. Nakajima, Y. Honda, O. Kitao, H. Nakai, T. Vreven, K. Throssell, J. A. Montgomery, Jr., J. E. Peralta, F. Ogliaro, M. Bearpark, J. J. Heyd, E. Brothers, K. N. Kudin, V. N. Staroverov, T. Keith, R. Kobayashi, J. Normand, K. Raghavachari, A. Rendell, J. C. Burant, S. S. Iyengar, J. Tomasi, M. Cossi, J. M. Millam, M. Klene, C. Adamo, R. Cammi, J. W. Ochterski, R. L. Martin, K. Morokuma, O. Farkas, J. B. Foresman, D. J. Fox, *Gaussian 09*, Gaussian, Inc.: Wallingford CT, 2016.

2 H. Su, K.-X. Zhang, B. Zhang, H.-H. Wang, Q.-Y. Yu, X.-H. Li, M. Antonietti, J.-S. Chen, *J. Am. Chem. Soc.*, 2017, **139**, 811–818.

3 R. V. Jagadeesh, H. Junge, M.-M. Pohl, J. Radnik, A. Brückner, M. Beller, *J. Am. Chem. Soc.*, 2013, **135**, 10776–10782.

4 Y.-X. Zhou, Y.-Z. Chen, L. Cao, J. Lu, H.-L. Jiang, *Chem. Commun.*, 2015, **51**, 8292–8295.

5 W. Zhong, H. Liu, C. Bai, S. Liao, Y. Li, *ACS Catal.*, 2015, **5**, 1850–1856.

6 D. S. Mannel, M. S. Ahmed, T. W. Root, S. S. Stahl, *J. Am. Chem. Soc.*, 2017, **139**, 1690–1698.

7 C. Liu, J. Wang, L. Meng, Y. Deng, Y. Li, A. Lei, *Angew. Chem., Int. Ed.*, 2011, **50**, 5144–5148.

8 Q. Xiao, Z. Liu, A. Bo, S. Zavahir, S. Sarina, S. Bottle, J. D. Riches, H. Zhu, *J. Am. Chem. Soc.*, 2015, **137**, 1956−1966.